Inorg. Chem. **2008**, *47*, 2133−2141

Inorganic Chemistry

Article

Thermodynamic, Kinetic, and Computational Study of Heavier Chalcogen (S, Se, and Te) Terminal Multiple Bonds to Molybdenum, Carbon, and Phosphorus

James E. McDonough,[†] Arjun Mendiratta,[‡] John J. Curley,[‡] George C. Fortman,[†] Serena Fantasia,[§] Christopher C. Cummins,[*,‡] Elena V. Rybak-Akimova,[*,||] Steven P. Nolan,[*,§] and Carl D. Hoff[*,†]

Department of Chemistry, University of Miami, 1301 Memorial Drive, Coral Gables, Florida 33146, Department of Chemistry, Massachusetts Institute of Technology, 77 Massachusetts Avenue, Cambridge, Massachusetts 02139-4307, Department of Chemistry, Tufts University, 62 Talbot Avenue, Medford, Massachusetts 02155, and Institute of Chemical Research of Catalonia (ICIQ), Av. Països Catalans 16, 43007, Tarragona, Spain

Received August 13, 2007

Enthalpies of chalcogen atom transfer to Mo(N[*t*-Bu]Ar)$_3$, where Ar = 3,5-$C_6H_3Me_2$, and to IPr (defined as *bis*-(2,6-isopropylphenyl)imidazol-2-ylidene) have been measured by solution calorimetry leading to bond energy estimates (kcal/mol) for EMo(N[*t*-Bu]Ar)$_3$ (E = S, 115; Se, 87; Te, 64) and EIPr (E = S, 102; Se, 77; Te, 53). The enthalpy of S-atom transfer to PMo(N[*t*-Bu]Ar)$_3$ generating SPMo(N[*t*-Bu]Ar)$_3$ has been measured, yielding a value of only 78 kcal/mol. The kinetics of combination of Mo(N[*t*-Bu]Ar)$_3$ with SMo(N[*t*-Bu]Ar)$_3$ yielding (μ-S)[Mo(N[*t*-Bu]Ar)$_3$]$_2$ have been studied, and yield activation parameters $\Delta H^{\ddagger} = 4.7 \pm 1$ kcal/mol and $\Delta S^{\ddagger} = -33 \pm 5$ eu. Equilibrium studies for the same reaction yielded thermochemical parameters $\Delta H^{\circ} = -18.6 \pm 3.2$ kcal/mol and $\Delta S^{\circ} = -56.2 \pm 10.5$ eu. The large negative entropy of formation of (μ-S)[Mo(N[*t*-Bu]Ar)$_3$]$_2$ is interpreted in terms of the crowded molecular structure of this complex as revealed by X-ray crystallography. The crystal structure of Te-atom transfer agent $TePCy_3$ is also reported. Quantum chemical calculations were used to make bond energy predictions as well as to probe terminal chalcogen bonding in terms of an energy partitioning analysis.

Introduction

The availability of thermochemical data for terminally bonded chalcogen substituents decreases as one descends the group 16 period.[1–4] In addition to this paucity of experimental data, theoretical understanding of the bonding to terminal chalcogen atom substituents similarly diminishes with increasing atomic number. Elucidation of the nature of terminal chalcogen bonding is an active area of investigation, with various formal bond orders being possible between the chalcogen atom and the fragment with which it interacts.[5–8]

The driving force for desulfurization of thiyl radicals by phosphines,[9,10] as shown in eq 1, is the exothermic formation of SPR'_3 via an intermediate thiophosphoranyl radical. Chalcogenyl radicals •ER (E = S, Se, or Te) can be generated by the interaction of disulfides with metal complexes[11,12] and could provide a reaction pathway for the thermal generation of alkyl radicals as shown in eq 2.

---

[*] To whom correspondence should be addressed. E-mail: ccummins@mit.edu.

[†] University of Miami.

[‡] Massachusetts Institute of Technology.

[§] ICIQ.

[||] Tufts University.

(1) Donahue, J. P. *Chem. Rev.* **2006**, *106*, 4747–4783.
(2) Holm, R. H.; Donahue, J. P. *Polyhedron* **1993**, *12*, 571–589.
(3) Mompean, F. J.; Perrone, J.; Illemassène, M. Chemical Thermodynamics of Selenium. *Chemical Thermodynamics*; Olin, Å., Noläng, B., Öhman, L.-O., Osadchii, E. G., Rosén, E., Eds. Elsevier: Amsterdam, 2005; Vol. *7*.
(4) Linstrom, P. J.; Mallard, W. G. *J. Chem. Eng. Data* **2001**, *46*, 1059–1063.
(5) Dobado, J. A.; Martínez-García, H.; Molina, J. M.; Sundberg, M. R. *J. Am. Chem. Soc.* **1998**, *120*, 8461–8471.
(6) Streitwieser, A.; Rajca, A.; McDowell, R. S.; Glaser, R. *J. Am. Chem. Soc.* **1987**, *109*, 4184–4188.
(7) González-Blanco, O.; Branchadell, V.; Monteyne, K.; Ziegler, T. *Inorg. Chem.* **1998**, *37*, 1744–1748.
(8) Cotton, F. A.; Feng, X. *Inorg. Chem.* **1996**, *35*, 4921–4925.
(9) Franz, J. A.; Bushaw, B. A.; Alnajjar, M. S. *J. Am. Chem. Soc.* **1989**, *111*, 268–275.
(10) Bentrude, W. G. *Acc. Chem. Res.* **1982**, *15*, 117–125.
(11) McDonough, J. E.; Weir, J. J.; Carlson, M. J.; Hoff, C. D.; Kryatova, O. P.; Rybak-Akimova, E. V.; Clough, C. R.; Cummins, C. C. *Inorg. Chem.* **2005**, *44*, 3127–3136.

10.1021/ic701611p CCC: $40.75

$$\bullet SR + PR'_3 \rightleftarrows \bullet[RSPR'_3] \rightleftarrows \bullet R + SPR'_3 \qquad (1)$$

$$0.5RSSR + ML_n \rightarrow RSML_n \rightarrow \bullet R + SML_n \qquad (2)$$

A complicating factor in the chemistry of the terminally bonded chalcogen atom is that, in addition to uncertainties in bond order assignment, such systems are prone to form dimers or higher oligomers. Exemplifying this is the dimerization chemistry of heteroaldehydes, illustrated in eq 3. The fact that four C−E "single bonds" are stronger than two C═E "double bonds" generally seems to drive equilibria of the type illustrated in eq 3 to form the cyclic dimer product, especially for the heavier Se and Te systems. In spite of this, several seleno- and telluro-aldehydes stabilized by coordination to a metal complex[13–15] or by the presence of a π-donor heteroatom[16] have yielded to synthesis. Stable compounds of formula $E{=}CR_2$ (E = Se or Te), with R as a simple hydrocarbyl substituent, are rare. As Power has written,[17] "The difficulty in preparing the heavy aldehydes and ketones probably does not arise from the weakness of the CE π bond. In fact π bonds between carbon (and to a certain extent silicon and germanium) and the heavier chalcogens are among the strongest π bonds between heavier elements. It seems probable that the lack of a steric hindrance at the chalcogen combined with the three-coordination at carbon renders these compounds particularly susceptible to further reaction."

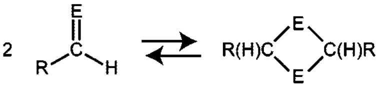

(3)

The apparent thermodynamic propensity for doubly bonded chalcogen−element systems to undergo dimerization extends to chalcogen−transition-element complexes. Formation of $[Cp_2{}^tZrTe]_2$ is proposed to occur by a loss of L from $Cp_2{}^t(L)ZrTe$.[18] Kuchta and Parkin[19] have prepared gallium(I) compounds encumbered by *tris*-pyrazolyl borate supporting ligands, for example, $[Tp^{t\text{-}Bu_2}]GaE$ (E = Se, Te), which are monomeric in contrast to their tetrameric permethyl cyclopentadienyl analogues, $[Cp^*GaE]_4$.[20] Physical study of the selenium atom transfer[21] reaction in eq 4 allowed derivation of the following thermodynamic parameters: $\Delta H = -6.8 \pm 0.7$ kcal/mol and $\Delta S = 9 \pm 2$ eu.[19]

$$[Tp^{Bu^t_2}]Ga + SePEt_3 \rightleftarrows [Tp^{Bu^t_2}]GaSe + PEt_3 \qquad (4)$$

Demonstrating our interest in chalcogen thermochemistry, we reported previously the enthalpies of chalcogen atom transfer forming the nonmetal compounds EYR_3 (E = S, Se, Te; Y = P, As, Sb; R = alkyl or aryl group).[21] Also reported was S-atom transfer to *N*-heterocyclic carbene (NHC) acceptors to form the corresponding thioureas.[22] These data provide estimates of absolute bond strengths involving the terminal chalcogen atom, and also they provide a basis for extension of such thermochemical information to a wider range of chalcogen atom acceptors. Of peripheral interest to this discussion is that enthalpies of S-atom insertion into the M−H bond of Cp− and fulvalene−metal hydride complexes have also been reported.[23,24]

The objective of the present work is to extend our understanding of terminal chalcogen bond thermochemistry to include the odd-electron complexes $EMo(N[t\text{-}Bu]Ar)_3$ (E = S, Se, and Te),[25] and also to extend the available data for chalcogen transfer to NHC acceptors to include Se and Te. The conversion of a sulfide ligand from a terminal to a bridging bonding mode is studied herein using both calorimetric and stopped-flow kinetic methods, and a single-crystal X-ray diffraction study is reported for the sulfide-bridged complex $(\mu\text{-}S)[Mo(N[t\text{-}Bu]Ar)_3]_2$. In order to gain access to clean Te-atom transfer reactions, the compound $TePCy_3$ was prepared, and its structural characterization is reported herein. Providing a contrast with typical phosphine S-atom acceptors, the terminal phosphide complex $PMo(N[t\text{-}Bu]Ar)_3$[26,27] is examined with regard to the thermochemistry of its conversion to $(SP)Mo(N[t\text{-}Bu]Ar)_3$,[28] a rare example of a terminal PS complex. To supplement the wealth of new experimental data reported herein, quantum chemical calculations were performed and are presented as an aid to our interpretation of the experimental facts.

Materials and Methods

All operations were performed under argon or nitrogen using standard Schlenk and glovebox techniques. Toluene and heptane were purified by distillation under argon from sodium benzophenone ketyl into flame-dried glassware. Methylene chloride was refluxed under argon over P_2O_5 and then distilled. Triphenylphosphine (PPh_3) and tricyclohexylphosphine (PCy_3) were obtained from Aldrich and recrystallized from toluene/heptane solutions. Triphenylantimony sulfide ($SSbPh_3$) was obtained from Aldrich and was used without

---

[12] McDonough, J. E.; Weir, J. J.; Sukcharoenphon, K.; Hoff, C. D.; Kryatova, O. P.; Rybak-Akimova, E. V.; Scott, B. C.; Kubas, G. J.; Stephens, F. H.; Mendiratta, A.; Cummins, C. C. *J. Am. Chem. Soc.* **2006**, *128*, 10295–10303.

[13] Minoura, M.; Kawashima, T.; Okazaki, R. *Tetrahedron Lett.* **1997**, *38*, 2501–2504.

[14] Fischer, H.; Stumpf, R.; Roth, G. In *Advances in Organometallic Chemistry*; Academic Press: San Diego, CA. 1999; Vol. 43, p 125–196.

[15] Okazaki, R.; Tokitoh, N. *Acc. Chem. Res.* **2000**, *33*, 625–630.

[16] Li, G. M.; Zingaro, R. A.; Segi, M.; Reibenspies, J. H.; Nakajima, T. *Organometallics* **1997**, *16*, 756–762.

[17] Power, P. P. *Chem. Rev.* **1999**, *99*, 3463–3503.

[18] Gindelberger, D. E.; Arnold, J. *Organometallics* **1994**, *13*, 4462–4468.

[19] Kuchta, M. C.; Parkin, G. *Inorg. Chem.* **1997**, *36*, 2492–2493.

[20] Schulz, S.; Andruh, M.; Pape, T.; Heinze, T.; Roesky, H. W.; Häming, L.; Kuhn, A.; Herbstirmer, R. *Organometallics* **1994**, *13*, 4004–4007.

[21] Capps, K. B.; Wixmerten, B.; Bauer, A.; Hoff, C. D. *Inorg. Chem.* **1998**, *37*, 2861–2864.

[22] Huang, J. K.; Schanz, H. J.; Stevens, E. D.; Nolan, S. P.; Capps, K. B.; Bauer, A.; Hoff, C. D. *Inorg. Chem.* **2000**, *39*, 1042–1045.

[23] Bauer, A.; Capps, K. B.; Wixmerten, B.; Abboud, K. A.; Hoff, C. D. *Inorg. Chem.* **1999**, *38*, 2136–2142.

[24] Capps, K. B.; Whitener, G. D.; Bauer, A.; Abboud, K. A.; Wasser, I. M.; Vollhardt, K. P. C.; Hoff, C. D. *Inorg. Chem.* **2002**, *41*, 3212–3217.

[25] Johnson, A. R.; Davis, W. M.; Cummins, C. C.; Serron, S.; Nolan, S. P.; Musaev, D. G.; Morokuma, K. *J. Am. Chem. Soc.* **1998**, *120*, 2071–2085.

[26] Laplaza, C. E.; Davis, W. M.; Cummins, C. C. *Angew. Chem., Int. Ed. Engl.* **1995**, *34*, 2042–2044.

[27] Stephens, F. H.; Johnson, M. J. A.; Cummins, C. C.; Kryatov, O. P.; Kryatov, S. V.; Rybak-Akimova, E. V.; McDonough, J. E.; Hoff, C. D. *J. Am. Chem. Soc.* **2005**, *127*, 15191–15200.

[28] Johnson, M. J. A.; Odom, A. L.; Cummins, C. C. *Chem. Commun.* **1997**, 1523–1524.

purification. Calorimetric measurements were performed in a Calvet calorimeter as previously described.[29]

Preparation of SPCy$_3$[30]. In the glovebox, PCy$_3$ (5.00 g, 17.8 mmol) was added to a flask with S$_8$ (0.57 g, 2.22 mmol, 1 equiv) and dissolved in toluene (20 mL). The solution was allowed to stir overnight, after which time the product precipitated. The mother liquor was decanted, and the crude product was dried under a vacuum. This crude product was extracted with toluene (100 mL), the extract was filtered, and the filtrate was reduced in volume to ca. 30 mL; the flask was then heated until the concentrated filtrate became homogeneous. After being allowed to cool to room temperature, the flask was placed in the freezer overnight. The product was then collected by filtration as large colorless crystals, which were washed with heptane (20 mL) and dried under a vacuum (2.85 g, 9.12 mmol, 51%). ^{31}P NMR: δ 62.44 ppm.

Preparation of SePCy$_3$[31]. This procedure was essentially identical to that described above for SPCy$_3$. The quantities used were as follows: PCy$_3$ (5.00 g, 17.8 mmol), elemental selenium (4.22 g, 53.4 mmol, 3 equiv). The yield of SePCy$_3$ was 1.919 g, 5.34 mmol, 30%. ^{31}P NMR: δ 59.10 ppm.

Preparation of TePCy$_3$ and Crystal Growth for X-Ray Determination. This procedure was essentially identical to that described above for EPCy$_3$ (E = S, Se).[32] The quantities used were as follows: PCy$_3$ (5.00 g, 17.8 mmol), ground elemental tellurium (11.38 g, 89.1 mmol, 5 equiv). The yield of TePCy$_3$ obtained as large, bright yellow, X-ray quality crystals was 4.55 g, 11.2 mmol, 62.5%. ^{31}P NMR: δ 29.21 ppm.

Preparation of (μ-S)[Mo(N[*t*-Bu]Ar)$_3$]$_2$. At −35 °C, a solution of Mo(N[*t*-Bu]Ar)$_3$[33,34] (271 mg, 0.434 mmol, 1 equiv) in Et$_2$O (10 mL) was added dropwise to a rapidly stirred solution of SMo(N[*t*-Bu]Ar)$_3$[25] (285 mg, 0.434 mmol, 1 equiv) in Et$_2$O (5 mL). Mixing of these two orange-brown solutions led to the rapid formation of a purple mixture. The mixture was stirred for 10 min before being concentrated, under a dynamic vacuum, to ca. 8 mL total volume. The resulting mixture was stored at −35 °C for 2 d, during which time a precipitate formed. The precipitate was collected by filtration as a purple powder that was washed with freshly thawed (−130 °C) *n*-pentane (5 mL × 2). Subsequent drying under a dynamic vacuum provided the product as a purple powder (240 mg, 0.186 mmol, 43.2%). The μ-sulfide complex (μ-S)[Mo(N[*t*-Bu]Ar)$_3$]$_2$ forms purple solutions when dissolved in organic solvents at −35 °C and brown solutions when dissolved in the same solvents at 20 °C. The brown solution is an equilibrium mixture containing Mo(N[*t*-Bu]Ar)$_3$, SMo(N[*t*-Bu]Ar)$_3$, and (μ-S)[Mo(N[*t*-Bu]Ar)$_3$]$_2$. ^{1}H NMR (400 MHz, d_8-toluene, −30 °C): δ 7.27 (s, 6H, *p*-Ar), 6.69 (s, 6H, *o*-Ar), 4.41 (s, 6H, *o*-Ar), 2.30 (s, 18H, ArC*H*$_3$), 2.05 (s, 18H, ArC*H*$_3$), 1.73 (s, 54H, NCC*H*$_3$). ^{13}C NMR (125 MHz, d_8-toluene, −8 °C): δ 152.9 (s, *ipso*-Ar), 136.3 (s, aryl), 136.0 (s, aryl), 133.9 (s, aryl), 133.6 (s, aryl), 127.9 (s, aryl), 66.2 (s, *C*CH$_3$), 33.6 (s, C*C*H$_3$), 22.4 (s, Ar-*C*H$_3$), 21.8 (s, Ar-CH$_3$). Combustion analysis for C$_{72}$H$_{108}$Mo$_2$N$_6$S, found (calc): C, 65.82 (67.48); H, 8.35 (8.49); N, 6.37 (6.56). Crystals for the X-ray diffraction study were obtained from a THF solution of (μ-S)[Mo(N[*t*-Bu]Ar)$_3$]$_2$ that had been stored at −35 °C.

Variable-Temperature NMR Study of (μ-S)[Mo(N[*t*-Bu]Ar)$_3$]$_2$. The μ-sulfide complex (μ-S)[Mo(N[*t*-Bu]Ar)$_3$]$_2$ (7.5 mg, 5.84 μmol) was dissolved in cold d_8-toluene (0.932 mL, −35 °C), and the solution was transferred into an NMR tube connected to a vacuum adapter. The headspace was removed from the NMR tube by briefly applying a dynamic vacuum, the solution was frozen in a liquid nitrogen bath, and the tube was then sealed with a torch. The sample was stored frozen until just prior to insertion into a cold (−30 °C) NMR probe. ^{1}H NMR spectra were collected at various temperatures in the following sequence: −30, −20, −10, 0, +10, +20, +30, +35, +25, +15, +5, and −5 °C. The ^{1}H NMR spectra so obtained are eight-scan spectra taken over a spectral width of −80 ppm to 80 ppm with a delay time of 16 s between scans. The sample was allowed 5–10 min at each new temperature to ensure that the mixture had sufficient time to equilibrate before the NMR measurement was performed. A MeOH ^{1}H NMR thermometer was used at all temperatures to calibrate the actual temperature at the sample.[35]

Stopped-Flow Kinetic Measurements. Kinetic measurements were performed at temperatures from −20 to +25 °C using a Hi-Tech Scientific (Salisbury, Wiltshire, U.K.) SF-43 Multi-Mixing CryoStopped-Flow Instrument in diode array and single wavelength modes. The stopped-flow instrument was equipped with stainless steel plumbing, a 1.00 cm stainless steel mixing cell with sapphire windows, and an anaerobic gas-flushing kit. The instrument was connected to an IBM computer with IS-2 Rapid Kinetic software (Hi-Tech Scientific). The temperature in the mixing cell was maintained to ±0.1 K, and the mixing time was 2 to 3 ms. The driving syringe compartment and the cooling bath filled with heptane (Fisher) were flushed with argon before and during the experiments, using anaerobic kit flush lines. All flow lines of the SF-43 instrument were extensively washed with degassed, anhydrous toluene before charging the driving syringes with reactant solutions. The solutions of SMo(N[*t*-Bu]Ar)$_3$ were prone to degradation in the stopped-flow lines and partially decomposed over several hours. Therefore, the precise concentration of this solution was not known during the measurements. In order to compensate for this problem, the reaction was studied under an excess (at least 10-fold) of the second reactant, Mo(N[*t*-Bu]Ar)$_3$, which was stable in the stopped-flow instrument over extended periods of time. The rate constants determined under these pseudo-first-order conditions did not depend on the concentration of SMo(N[*t*-Bu]Ar)$_3$. Data analysis was performed with IS-2 Rapid Kinetic software from Hi-Tech Scientific, or Spectfit/32 Global Analysis System software from Biologic. Single-exponential kinetic profiles were observed in all experiments.

Computational Studies. All calculations were carried out on an eight-processor Quantum Cube computer from parallel quantum solutions.[36] The software employed was the ADF program suite;[37] the version, functionals, and basis sets are as described earlier[27] or as stated in the text.

Results and Discussion

Earlier sulfur-atom transfer studies reported by one of us were based largely on the use of the S-atom transfer reagent

---

(29) Stephens, F. H.; Figueroa, J. S.; Cummins, C. C.; Kryatova, O. P.; Kryatov, S. V.; Rybak-Akimova, E. V.; McDonough, J. E.; Hoff, C. D. *Organometallics* **2004**, *23*, 3126–3138.

(30) Issleib, K.; Brack, A. *Z. Anorg. Allg. Chem.* **1954**, *277*, 258–70.

(31) Zingaro, R. A.; McGlothlin, R. E. *J. Chem. Eng. Data* **1963**, *8*, 226–9.

(32) Zingaro, R. A. *J. Organomet. Chem.* **1963**, *1*, 200.

(33) Laplaza, C. E.; Odom, A. L.; Davis, W. M.; Cummins, C. C.; Protasiewicz, J. D. *J. Am. Chem. Soc.* **1995**, *117*, 4999–5000.

(34) Laplaza, C. E.; Johnson, M. J. A.; Peters, J. C.; Odom, A. L.; Kim, E.; Cummins, C. C.; George, G. N.; Pickering, I. J. *J. Am. Chem. Soc.* **1996**, *118*, 8623–8638.

(35) Ammann, C.; Meier, P.; Merbach, A. E. *J. Magn. Reson.* **1982**, *46*, 319–321.

(36) Parallel Quantum Solutions. http://www.pqs-chem.com (accessed Dec 2007).

(37) te Velde, G.; Bickelhaupt, F. M.; Baerends, E. J.; Fonseca Guerra, C.; van Gisbergen, S. J. A.; Snijders, J. G.; Ziegler, T. *J. Comput. Chem.* **2001**, *22*, 931–967.

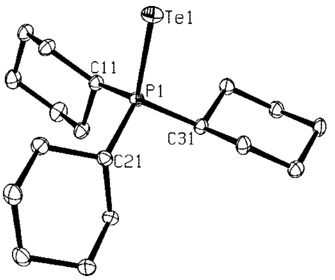

Figure 1. Molecular structure of TePCy$_3$ with ellipsoids drawn at the 50% probability level. See text for key metrical parameters.

SSbPh$_3$.[21] This compound is useful for calorimetric measurements of single S-atom transfer since it is a solid, the side product produced following S atom delivery (SbPh$_3$) is a relatively weakly coordinating ligand, and the formation of di- or polysulfide side-products is minimized compared to using S$_8$. Prior measurements of Se and Te transfer calorimetry were based on elemental Se and Te, which can be obtained in semiconductor grade purity but which react slowly due to limited solubility. While this slow reactivity could be tolerated in calorimetry studies involving complexes with supporting phosphine ligands, preliminary data for reactions with Mo(N[*t*-Bu]Ar)$_3$ and the elemental chalcogens did not appear promising. Therefore, calorimetric measurements of Se and Te atom transfer were based on reactions of the readily prepared and purified reagents SePCy$_3$ and TePCy$_3$. The latter reagents offer practical handling advantages over liquids such as SeP(*n*-Bu)$_3$ and TeP(*n*-Bu)$_3$, and the enthalpies of chalcogen atom transfer are identical within experimental error if based on SePCy$_3$ or SeP(*n*-Bu)$_3$, provided all species are in solution.[21] While conducting this work, we realized that the crystal structure of TePCy$_3$ had not been reported.[38,39] Therefore crystals of TePCy$_3$ were prepared, and the crystal structure was solved; the structural study is summarized in Figure 1. The compound is essentially tetrahedral at phosphorus with average Te−P−C angles of 111° and average C−P−C angles of 109°. The Te−P interatomic distance was found to be 2.3632(7) Å. In comparison, the crystal structure study of TeP(*t*-Bu)$_3$ revealed very similar parameters at phosphorus: a Te−P distance of 2.368 Å, average Te−P−C angles of 109°, and average C−P−C angles of 110°.

The reaction of Mo(N[*t*-Bu]Ar)$_3$ with TePCy$_3$ is rapid and occurs quantitatively as shown in eq 5. The enthalpy of the reaction corresponding to eq 5 was measured on the basis of the solid reagent as -8.3 ± 0.5 kcal/mol and is corrected by the endothermic enthalpy of solution of TePCy$_3$ in toluene of $+4.1 \pm 0.5$ kcal/mol to give a final value of -12.4 ± 1.0 kcal/mol with all species in toluene solution.

$$\mathrm{Mo(N[}t\text{-}\mathrm{Bu]Ar)_3 + TePCy_3 \rightarrow TeMo(N[}t\text{-}\mathrm{Bu]Ar)_3 + PCy_3} \quad (5)$$

In studying the calorimetry of eq 5, we used TePCy$_3$ as the limiting reagent, while Mo(N[*t*-Bu]Ar)$_3$ was present in excess. No signs of interaction between product TeMo(N[*t*-Bu]Ar)$_3$ and excess Mo(N[*t*-Bu]Ar)$_3$ were found at room temperature. As a check on the measurements for eq 5, similar measurements were performed on the reaction corresponding to eq 6 with TeP(*n*-Bu)$_3$ as the Te-atom transfer agent.

Table 1. Experimental Enthalpies of Chalcogen Atom (E = S, Se, or Te) Transfer,[a] and Derived Bond Dissociation Enthalpies

E atom donor	acceptor	ΔH_{rxn}	bond, BDE
SSbPh$_3$[b]	[**Mo**][d]	−47.9 (0.7)	S−Mo, 115
SSbPh$_3$	P[**Mo**][d]	−11.4 (1.2)	S−P, 78
SSbPh$_3$[c]	PPh$_3$	−21.5 (1.1)	S−P, 88
SP[**Mo**][d]	PPh$_3$	−11.5 (1.2)	S−PMo, 78
SePCy$_3$	[**Mo**][d]	−11.7 (1.0)	Se−Mo, 87
SePCy$_3$	IPr	−2.0 (0.4)	Se−C, 77
TePCy$_3$	[**Mo**][d]	−12.4 (1.1)	Te−Mo, 64
TePCy$_3$	IPr	−0.6 (0.3)	Te−C, 53

[a] All data are given in units of kcal/mol and are for all species in toluene solution. BDE estimates are believed to be reliable to within ± 3 kcal/mol. [b] Data for this reaction are corrected to reflect formation of the terminal sulfide complex, SMo(N[*t*-Bu]Ar)$_3$, as discussed in the text. [c] This measurement was in accord with a previously reported experimental value.[21] [d] Here, [**Mo**] is the abbreviation for Mo(N[*t*-Bu]Ar)$_3$.

$$\mathrm{Mo(N[}t\text{-}\mathrm{Bu]Ar)_3 + TeP(}n\text{-}\mathrm{Bu)_3 \rightarrow TeMo(N[}t\text{-}\mathrm{Bu]Ar)_3 + P(}n\text{-}\mathrm{Bu)_3} \quad (6)$$

The enthalpy of reaction obtained for eq 6 based on solid Mo(N[*t*-Bu]Ar)$_3$ as the limiting reactant was -12.2 ± 1.2 kcal/mol. Data based on eq 5 are believed to be more reliable due to difficulty in handling samples of solid Mo(N[*t*-Bu]Ar)$_3$without some loss of activity. Using a value of 52 kcal/mol for the Te−P bond energy in TePCy$_3$[21] yields a value of 64 kcal/mol for the formation of the Mo−Te bond in TeMo(N[*t*-Bu]Ar)$_3$.

In contrast to the relatively rapid reaction of Mo(N[*t*-Bu]Ar)$_3$ with TePCy$_3$, the analogous reaction with SePCy$_3$ was much slower. Furthermore, the mixing of Mo(N[*t*-Bu]Ar)$_3$ with SPCy$_3$ led to no sign of reaction over 6 h at 30 °C. The latter observation is in keeping with the work of Johnson and co-workers, who found that the kinetic ability of Mo(N[*t*-Bu]Ar)$_3$ to desulfurize SPPh$_3$ as well as metal thiocarbonyl compounds was shown to be drastically diminished relative to that of the related molybdaziridine hydride complex, Mo(H)(η^2-Me$_2$C=NAr)(N[*i*-Pr]Ar)$_2$, which serves as a synthon for Mo(N[*i*-Pr]Ar)$_3$.[40]

In spite of the slow nature of the reaction of Mo(N[*t*-Bu]Ar)$_3$ with SePCy$_3$, accurate calorimetry data for this reaction were obtained and led to a derived value of 87 kcal/mol for the Mo−Se bond energy in SeMo(N[*t*-Bu]Ar)$_3$. This value is obtained using 75 kcal/mol for the Se−PCy$_3$ bond dissociation energy (BDE).[21] Bond energies are also collected and presented in Table 1.

Enthalpy of Formation of SMo(N[*t*-Bu]Ar)$_3$ and (μ-S)[Mo(N[*t*-Bu]Ar)$_3$]$_2$. The enthalpy of S-atom transfer to Mo(N[*t*-Bu]Ar)$_3$ was investigated previously using ethylene sulfide as the S-atom transfer reagent.[25] In the present work, this was repeated using SSbPh$_3$ as the S-atom source.

---

(38) Kuhn, N.; Schumann, H.; Wolmershauser, G. *Z. Naturforsch., B: Chem. Sci.* **1987**, *42*, 674–678.

(39) Kuhn, N.; Henkel, G.; Schumann, H.; Fröhlich, R. *Z. Naturforsch., B: Chem. Sci.* **1990**, *45*, 1010–1018.

(40) Caskey, S. R.; Stewart, M. H.; Kivela, J. E.; Sootsman, J. R.; Johnson, M. J. A.; Kampf, J. W. *J. Am. Chem. Soc.* **2005**, *127*, 16750–16751.

Initial measurements of the enthalpy of S-atom transfer in which $SSbPh_3$ was the limiting reagent and excess Mo(N[*t*-Bu]Ar)$_3$ was present in solution did not give reproducible results, and also the data indicated greater exothermicity when more concentrated solutions of Mo(N[*t*-Bu]Ar)$_3$ were employed. This suggested that the following two reactions occurred during the calorimetric measurements:

$$\mathrm{Mo(N[}t\mathrm{\text{-}Bu]Ar)_3 + SSbPh_3 \rightarrow SMo(N[}t\mathrm{\text{-}Bu]Ar)_3 + SbPh_3} \quad (7)$$

$$\mathrm{Mo(N[}t\mathrm{\text{-}Bu]Ar)_3 + SMo(N[}t\mathrm{\text{-}Bu]Ar)_3 \rightleftarrows (}\mu\mathrm{\text{-}S)[Mo(N[}t\mathrm{\text{-}Bu]Ar)_3]_2} \quad (8)$$

Thus, the observed enthalpies of reaction included not only the exothermic contribution from S-atom transfer (eq 7) but also the secondary contribution from the condensation reaction described by eq 8. The more exothermic enthalpies of reaction in concentrated solutions of Mo(N[*t*-Bu]Ar)$_3$ accordingly are attributed to the exothermic formation of (μ-S)[Mo(N[*t*-Bu]Ar)$_3$]$_2$ in varying amounts. Variable-temperature NMR studies allowing determination of K_{eq} for the equilibrium described by eq 8 were performed in C_6D_6. Plots of $\ln(K_{\mathrm{eq}})$ versus reciprocal temperature (Figure S1, Supporting Information) yielded thermodynamic parameters $\Delta H° = -18.6 \pm 3.2$ kcal/mol and $\Delta S° = -56.2 \pm 10.5$ eu for the reversible formation of the sulfide-bridged complex (μ-S)[Mo(N[*t*-Bu]Ar)$_3$]$_2$.

Use of the equilibrium data corresponding to eq 8 allowed correction of the calorimetric data obtained for the reactions corresponding to eqs 7 and 8 combined, in varying degrees, to yield a derived value of $\Delta H = -47.9 \pm 0.7$ kcal/mol for the S-atom transfer reaction of eq 7, and therefore to yield a value of 115 kcal/mol for the terminal molybdenum−sulfide bond in SMo(N[*t*-Bu]Ar)$_3$. This value is higher than that derived earlier (104 kcal/mol) from a calorimetric study of the reaction of ethylene sulfide with Mo(N[*t*-Bu]Ar)$_3$.[25]

Formation of the μ-sulfide complex (eq 8) can be viewed in the formal sense as a reaction in which a terminal molybdenum−sulfur double bond is replaced by the two single bonds that link the bridging sulfur atom to the two molybdenum centers in the product. Since this reaction has $\Delta H° = -18.6 \pm 3.2$ kcal/mol and the terminal S−Mo BDE estimated in this work is 115 kcal/mol, it follows that the estimated average S−Mo single bond BDE in (μ-S)[Mo(N[*t*-Bu]Ar)$_3$]$_2$ is ca. 67 kcal/mol. The latter value can be compared to the recently reported value (55 kcal/mol) of the S−Mo BDE for the benzenethiolate complex PhSMo(N[*t*-Bu]Ar)$_3$.[12] This comparison is made with the following caveat: unlike the simple single-for-double bond exchange process indicated by the RC(E)H dimerization illustrated in eq 3, the formation of the present μ-sulfide complex is also a redox process in which molybdenum(III) and molybdenum(V) combine to give two molybdenum(IV) centers; this redox comproportionation doubtless contributes to the observed thermochemistry to a degree that is difficult to assess. An additional use of these data was made to estimate the energy of phenyl radical generation by carbon−sulfur bond homolysis as indicated in eq 9:

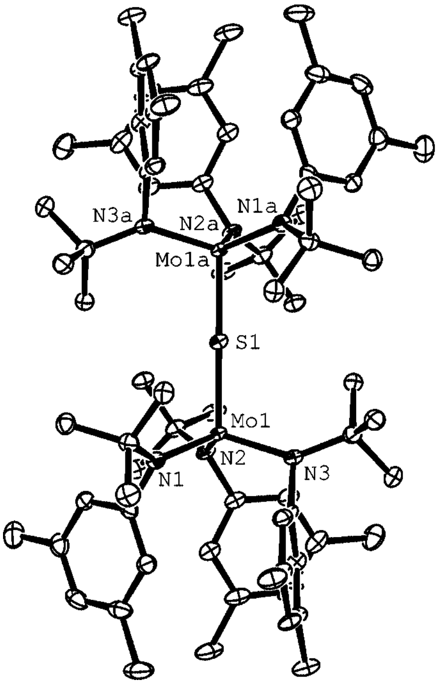

Figure 2. Molecular structure of (μ-S)[Mo(N[*t*-Bu]Ar)$_3$]$_2$ with ellipsoids drawn at the 50% probability level. See text for key metrical parameters.

$$\mathrm{PhSMo(N[}t\mathrm{\text{-}Bu]Ar)_3 \rightarrow {\bullet}Ph + SMo(N[}t\mathrm{\text{-}Bu]Ar)_3} \quad (9)$$

Using the literature value of 88.5 ± 1.5 kcal/mol for the carbon−sulfur BDE for the $\bullet SC_6H_5$ radical[41] leads to an estimated value for ΔH_{rxn} for the fragmentation reaction in eq 9 of approximately +29 kcal/mol.

Molecular Structure of (μ-S)[Mo(N[*t*-Bu]Ar)$_3$]$_2$. The equilibrium represented by eq 8 is shifted to favor formation of the dinuclear sulfide-bridged complex at lower temperatures, and the storage of sealed tubes in a freezer yielded crystals of (μ-S)[Mo(N[*t*-Bu]Ar)$_3$]$_2$ that were suitable for a single-crystal X-ray diffraction study. The structure so obtained is shown in Figure 2.

The sulfur atom in the structure of (μ-S)[Mo(N[*t*-Bu]Ar)$_3$]$_2$ is skewered by a crystallographically imposed C_2 axis. This axis relates the two molybdenum-containing halves of the molecule. Both Mo−S distances are 2.2025(4) Å, while the Mo−S−Mo angle is 178.09(6)°. The *tert*-butyl groups of opposing molybdenum centers are interdigitated with respect to one another, a circumstance consonant with minimization of unfavorable steric repulsions involving these substituents.[42] It should be noted that the crowded solid-state structure of the μ-sulfide complex is consistent with this complex's solution ^{1}H NMR spectrum, in that separate signals are observed for equatorial and axial aryl methyl groups, and also for the inequivalent ortho protons on each aryl ring. Each half of the molecule is C_3 symmetric on the NMR time scale, and unlike the case for less-crowded mononuclear systems (e.g., NMo(N[*t*-Bu]Ar)$_3$), the two

---

(41) Benson, S. W. *Chem. Rev.* **1978**, *78*, 23–35.

(42) Johnson, M. J. A.; Lee, P. M.; Odom, A. L.; Davis, W. M.; Cummins, C. C. *Angew. Chem., Int. Ed. Engl.* **1997**, *36*, 87–91.

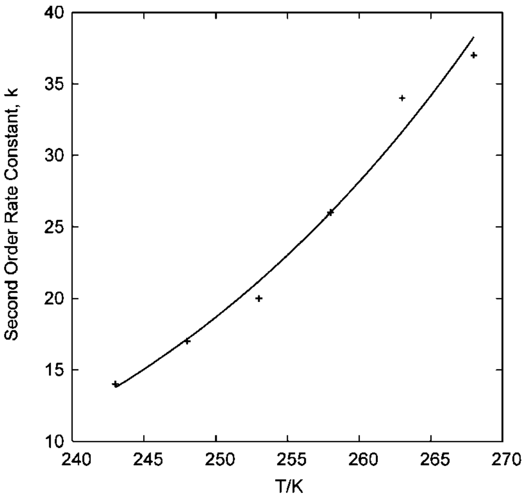

Figure 3. Plot of second-order rate constants, *k*, versus temperature along with least-squares fit to the exponential form of the Eyring equation. The rate constants are for the formation of (μ-S)[Mo(N[*t*-Bu]Ar)$_3$]$_2$. See the text for discussion of the activation parameters.

possible C_3 enantiomers are not undergoing interconversion on this time scale. Such frozen-out behavior has been seen previously for the analogous μ-phosphide-bridged dinuclear complex (μ-P)[Mo(N[*t*-Bu]Ar)$_3$]$_2$.[27,42]

Kinetic Study of μ-Sulfide Complex Formation. The rate of dinuclear μ-sulfide complex formation (corresponding to the forward reaction in eq 8) was investigated by a stopped-flow kinetic study. Spectroscopic changes that accompany this reaction are shown in Supporting Information Figure 2. The data were fit to a process first-order in each reactant. An Eyring treatment of derived values for the second-order rate constants for the reaction, shown in Figure 3, yielded activation parameters $\Delta H^{\ddagger} = 4.7 \pm 1$ kcal/mol and $\Delta S^{\ddagger} = -33 \pm 5$ eu. These values can be compared to those we reported earlier[27] for equilibrium formation of the analogous μ-phosphide system, a reaction portrayed in eq 10.

$$\mathrm{Mo(N[}t\text{-}\mathrm{Bu]Ar)_3} + \mathrm{PMo(N[}t\text{-}\mathrm{Bu]Ar)_3} \rightleftarrows (\mu\text{-P})[\mathrm{Mo(N[}t\text{-}\mathrm{Bu]Ar)_3}]_2 \qquad (10)$$

Equilibrium studies of μ-phosphide formation (eq 10) revealed a more exothermic formation of the μ-P complex, as compared with the μ-S system, but they also revealed a more unfavorable entropy of formation: $\Delta H_{\mathrm{rxn}} = -20.7 \pm 0.4$ kcal/mol and $\Delta S_{\mathrm{rxn}} = -69.4 \pm 15$ eu. Activation parameters obtained for eq 10 were as follows:[27] $\Delta H^{\ddagger} = 3.3 \pm 1$ kcal/mol and $\Delta S^{\ddagger} = -38 \pm 8$ eu. Thus, the forward rate of μ-sulfide dinuclear complex formation (eq 8) has an enthalpy of activation that is only ca. 2 kcal/mol greater than is the case for μ-phosphide formation (eq 10). Also, the observed entropies of activation are quite similar in magnitude, being large and negative, for formation of both the μ-P and the μ-S complexes, in agreement with the associative nature of the reactions 8 and 10. The activation entropies for both bridge-forming reactions may be modulated by the unfavorable aspect of bringing in close proximity two large Mo(N[*t*-Bu]Ar)$_3$ fragments. The corresponding loss of many degrees of freedom is even more pronounced in the total reaction entropy, which reaches −56 eu for a larger sulfide bridge and −69 eu for a smaller phosphide bridge.

Scheme 1. Thermochemical Cycle with All Species in Solution for a Set of Three S-Atom Transfer Reactions (Experimentally Obtained Reaction Enthalpies Are Given in kcal/mol)

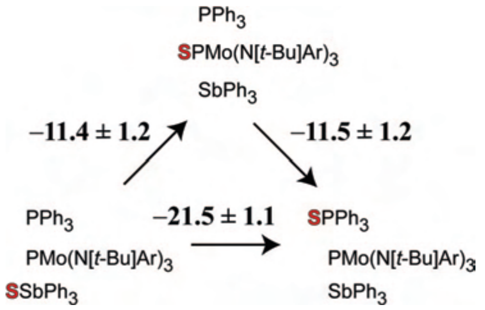

Sulfur Atom Transfer to the Terminal Phosphide Complex: Energy of PS Ligand Formation. In addition to chalcogen atom transfer to metal centers, the energetics of chalcogen transfer to and from main group and metal-bound main group centers is of interest. In this regard, it was of interest to determine the enthalpy of the S-atom transfer reactions outlined in Scheme 1.

Reaction of SSbPh$_3$ and PMo(N[*t*-Bu]Ar)$_3$ occurs cleanly and is moderately exothermic as shown in Scheme 1. The relatively weak S−P bond formed in the terminal PS complex SPMo(N[*t*-Bu]Ar)$_3$, however, is readily desulfurized by PPh$_3$. Reasonable agreement of the data presented in Scheme 1 was confirmed by repeating measurement of reaction of SSbPh$_3$ and PPh$_3$. The formal S−P bond energy in SPMo(N[*t*-Bu]Ar)$_3$ of 78 kcal/mol is the weakest S−P bond (wherein a 1-coordinate sulfur atom is bonded to phosphorus) reported to date[21] and some 20 kcal/mol weaker than those reported for trialkyl phosphine sulfides as exemplified by SPCy$_3$.

Enthalpies of Se and Te Atom Transfer to *N*-Heterocyclic Carbenes. In view of the scarcity of thermochemical data for the chalcogenocarbonyl (E−CR$_2$) bond, it was of interest to measure the enthalpies of the reactions illustrated in eq 11.

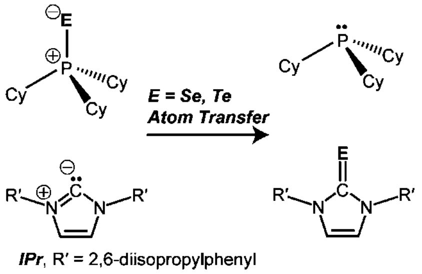

(11)

NMR studies showed that the chalcogen atom transfer was rapid and quantitative for E = Te, and occurred slowly for E = Se. Calorimetric data shown in Table 1 led to estimates for the formal double bonds between carbon in the Arduengo-type carbene and Se and Te of 77 and 53 kcal/mol, respectively. These data can be compared to our earlier reported value of 102 kcal/mol for the bond between S and

Table 2. Computational Study of Bonds to Terminal Chalcogen Substituents[a]

	isogyric reaction	$\Delta_r H^0$
12	$OCH_2 + {}^3[CH_2] \rightarrow C_2H_4 + {}^3[O]$	+16.1
13	$SCH_2 + {}^3[CH_2] \rightarrow C_2H_4 + {}^3[S]$	−42.3
14	$SeCH_2 + {}^3[CH_2] \rightarrow C_2H_4 + {}^3[Se]$	−64.6
15	$TeCH_2 + {}^3[CH_2] \rightarrow C_2H_4 + {}^3[Te]$	−86.9
16	$OPMe_3 + C(NHCH)_2 \rightarrow PMe_3 + OC(NHCH)_2$	−10.2
17	$SPMe_3 + C(NHCH)_2 \rightarrow PMe_3 + SC(NHCH)_2$	−9.4
18	$SePMe_3 + C(NHCH)_2 \rightarrow PMe_3 + SeC(NHCH)_2$	−7.0
19	$TePMe_3 + C(NHCH)_2 \rightarrow PMe_3 + TeC(NHCH)_2$	−7.4

bond	D_0	bond	D_0
$O-CH_2$	190.5	$O-C(NHCH)_2$	140.2
$S-CH_2$	132.1	$S-C(NHCH)_2$	90.0
$Se-CH_2$	109.8	$Se-C(NHCH)_2$	70.6
$Te-CH_2$	87.5	$Te-C(NHCH)_2$	51.4

[a] All data are given in units of kcal/mol and are for all species in the gas phase at 0 K.

IMes,[43] *bis*(2,4,6-trimethylphenyl) imidazol-2-ylidene, a carbene having electronic properties similar to those of the IPr carbene employed here.

Quantum Chemical Analysis of Bonding to Terminal Chalcogen Atom Substituents. The bonding in Arduengo-type carbenes and their derivatives is complex,[44] and the N-atom lone electron pairs of the imadazole ring play a role in stabilizing both the carbene and its chacogen-atom adduct. This in turn affects the thermochemistry of atom transfer reactions in which these *N*-heterocyclic carbenes are involved. In order to probe these factors, we turned to quantum chemical methods for the calculation of bonding parameters for simple ECH_2 and $EC(NHCH)_2$ model systems.

To estimate the E−C bond dissociation enthalpies at 0 K for the formaldehyde derivatives ECH_2 as a function of the chalcogen atom, the species required for the isogyric[45] eqs 12–15 in Table 2 were optimized using ADF with an all-electron TZ2P, ZORA relativistic basis set. The OLYP nonhybrid functional was employed;[46] this functional has been found recently to result in a typical average error that is significantly smaller than what is encountered for the BP86 nonhybrid functional.[47]

Frequencies were determined for the polyatomic species in reactions 12–15, and zero-point energy corrections were applied. The reaction enthalpies $\Delta_r H^0$ give the amount by which the E−C bond differs in energy with respect to the C−C bond bond in ethylene. In turn, the value of the C−C bond dissociation enthalpy for ethylene can be calculated with consideration of the known enthalpies of formation of ethylene and ${}^3[CH_2]$ at 0 K to be $D_0 = 174.4$ kcal/mol.[48] The latter number can be compared with the experimentally obtained ethylene C−C BDE at 298 K: 174.1 ± 0.3 kcal/mol. D_0 values for the four E−C bonds of eqs 12–15 are obtained by addition of the four $\Delta_r H^0$ values to the D_0 value for ethylene as shown in Table 2.

The results in Table 2 can be compared to experimental data in the literature. In the case of formaldehyde, the O−C BDE can be calculated from known enthalpies of formation to be $D_0 = 180.59$ kcal/mol, a number to be compared with a reported $D_{298} = 178.8 \pm 0.2$ kcal/mol.[49] Our computed value of 190.5 kcal/mol for the formaldehyde D_0 is therefore ca. 10 kcal/mol too high. It is worth noting that use of the BP86 functional in place of OLYP gave a corresponding value that was high by 20 kcal/mol. It has been noted that OLYP gives average errors on the order of 8.5 kcal/mol for molecules in the G3/99 test set.[47] If the trend of error in our calculation of D_0 for the ECH_2 molecules is assumed to be systematic, then the values shown in Table 2 are inflated by some 10 kcal/mol.

As a further test, the G3 enthalpy of formation of SCH_2 has recently been given as 27.68 kcal/mol,[50] permitting D_0 for its S−C linkage to be estimated as 132.6 kcal/mol. It is likely fortuitous that this value is almost an exact match to our OLYP-derived value of 132.1 kcal/mol, reported in Table 2.

As discussed above, it is expected that the E−C bonds in NHC E-atom adducts should be weak relative to corresponding bonds in ECH_2 systems. Since NHC systems are ground-state singlets, a different set of isogyric reactions must be used to estimate E−C bond energies in the urea analogs $E(NHCH)_2$. Given that a principal application for the NHC is as a phosphine substitute in homogeneous catalysis, and given also that the set of phosphine−chalcogen bond energies in $EPMe_3$ molecules have been computed and reported by Ziegler,[45] eqs 16–19 in Table 2 were selected for computation. The $\Delta_r H^0$ values computed for these reactions represent a competition between the NHC, here approximated with the model system $C(NHCH)_2$, and PMe_3 for the E atom. For each E atom, the NHC is more strongly bound than is PMe_3 by some 7–10 kcal/mol. As expected, the E−C bonds in the urea analogs are predicted to be weaker, by some 40 kcal/mol, than are the corresponding E−C bonds in the formaldehyde analogs. The absolute values of D_0 given here for the E−C bonds in the $EC(NHCH)_2$ molecules are pinned to the calculated values reported by Ziegler for the $EPMe_3$ phosphine chalcogenides.[45]

It is of crucial interest to compare the calculated reaction enthalpies for the isogyric reaction of $EPMe_3$ and the NHC model fragment $C(NHCH)_2$ with the experimental data determined in toluene solution. For these reactions, in which all species are soluble in toluene, it is expected that solvation effects will largely cancel, and so it is reasonable to compare computed gas-phase data with experimental solution-phase data. For SPR_3, earlier studies have given S−P bond strength estimates (kcal/mol) of 98 ($R = C_6H_{11}$), 96 ($R = C_4H_9$), and 94 ($R = CH_3$), and they have put forward 102 kcal/mol

---

(43) Dorta, R.; Stevens, E. D.; Scott, N. M.; Costabile, C.; Cavallo, L.; Hoff, C. D.; Nolan, S. P. *J. Am. Chem. Soc.* **2005**, *127*, 2485–2495.

(44) Hu, X. L.; Castro-Rodriguez, I.; Olsen, K.; Meyer, K. *Organometallics* **2004**, *23*, 755–764.

(45) *Computational thermochemistry: prediction and estimation of molecular thermodynamics*; Irikura, K. K., Frurip, D. J., Eds.; American Chemical Society: Washington, DC, 1998; ACS symposium series, 677.

(46) Handy, N. C.; Cohen, A. J. *Mol. Phys.* **2001**, *99*, 403–412.

(47) Curtiss, L. A.; Redfern, P. C.; Raghavachari, K. *J. Chem. Phys.* **2005**, 123.

(48) Curtiss, L. A.; Raghavachari, K.; Redfern, P. C.; Pople, J. A. *J. Chem. Phys.* **1997**, *106*, 1063–1079.

(49) Blanksby, S. J.; Ellison, G. B. *Acc. Chem. Res.* **2003**, *36*, 255–263.

(50) Gomes, J. R. B.; da Silva, M. *J. Phys. Chem. A* **2004**, *108*, 11684–11690.

Table 3. Energy Partitioning Analysis of Bonds to a Terminal Sulfur Atom[a]

	SCH_2 (C_{2v})[b]	SCH_2 (C_{2v})[c]	$SPMe_3$ (C_{3v})[c]
ΔE_{int}	−170.62	−199.84	−133.54
ΔE_{Pauli}	290.98	388.13	291.34
ΔE_{elstat}	−168.94	−242.05	−170.28
ΔE_{orb}	−292.66	−345.93	−254.60
	−204.84 (A_1)	−236.96 (A_1)	−207.30 (A_1)
	0.00 (A_2)	0.00 (A_2)	0.02 (A_2)
	−14.98 (B_1)	−16.10 (B_1)	−47.33 (E)
	−72.84 (B_2)	−92.87 (B_2)	

	$SNb(NH_2)_3$ (C_{3v})[c]	$SPMo(NH_2)_3$ (C_{3v})[c]	$SC(HNCH)_2$ (C_{2v})[c]
ΔE_{int}	−199.79	−119.34	−142.10
ΔE_{Pauli}	319.07	246.51	344.37
ΔE_{elstat}	−197.10	−105.13	−221.04
ΔE_{orb}	−321.76	−260.72	−265.43
	−275.22 (A_1)	−201.83 (A_1)	−213.72 (A_1)
	0.07 (A_2)	0.01 (A_2)	−0.13 (A_2)
	−46.62 (E)	−58.90 (E)	−16.98 (B_1)
			−34.61 (B_2)

[a] All data are given in units of kcal/mol and are for all species in the gas phase at 0 K. [b] Computed from interaction of neutral triplet fragments. [c] Computed from interaction of neutral singlet fragments.

for the S−C bond strength in SIMes. The foregoing yield an estimate of −8 kcal/mol for S atom transfer from $SPMe_3$ to IMes. This is in excellent agreement with the computed value of −9.4 kcal/mol as presented in Table 2. The experimental data for E-atom transfer from $EPCy_3$ to IPr (IMes in the case of E = S) are calculated on the basis of experimental data in solution to be E = S, −5.4; Se, −2.0; Te, −0.6 kcal/mol. The latter numbers should be compared with those obtained by quantum chemical calculations on the model systems (Table 2).

Energy Partitioning Analysis of Bonds to the Terminal S-Atom Substituent. The energy partitioning analysis scheme introduced independently by Morokuma[51] and by Ziegler and Rauk[52] has been applied profitably by Frenking et al.[53,54] to tease apart the factors that contribute to the energy of chemical bonds. In this scheme, the overall interaction energy between two fragments, ΔE_{int}, is given as the sum of three terms: $\Delta E_{Pauli} + \Delta E_{elstat} + \Delta E_{orb}$. Two of these terms ($\Delta E_{elstat} + \Delta E_{orb}$) are typically attractive and contribute to bonding, while the other, ΔE_{Pauli}, is repulsive. Calculation of the interaction energy and its components is carried out using the minimized geometry of the molecule of interest; thus, ΔE_{int} is generally larger than the bond dissociation enthalpy because the interacting fragments have not been permitted to relax to their ground electronic and geometric structures. We now apply such an analysis to the particular case of terminal bonds to a sulfur atom. As in the previous section, our computational method is density functional theory at the OLYP/TZ2P level as implemented in the ADF program suite.[37]

Five molecules having terminal bonds to sulfur were selected for analysis, as presented in Table 3. To illustrate the effect that the choice of fragments has upon the results obtained,[53] the particular case of thioformaldehyde (SCH_2) was computed from two different starting points. First, SCH_2 was considered to arise from interaction of a triplet sulfur atom having the configuration $[Ne](3s)^2(3p_x)^2(3p_y)^1(3p_z)^1$ with triplet methylene $^3[CH_2]$. This choice of fragments is a natural one for SCH_2 because there is a good correspondence with the ground-state electronic and geometric structures. However, an alternative is to consider the carbon−sulfur bond as a donor–acceptor interaction ($H_2C{:}\!\rightarrow S$) in which a singlet methylene fragment acts as a σ donor to a σ-acceptor sulfur atom; in this case, the π bond arises from donation of a sulfur lone pair (filled $3p_y$ orbital) to the out-of-plane empty p orbital of the singlet methylene fragment. In this case, the sulfur atom has the configuration $[Ne](3s)^2(3p_x)^2(3p_y)^2(3p_z)^0$ corresponding to the ^1S excited-state of atomic sulfur.[55] It can be seen (second entry in Table 3) that the overall interaction energy ΔE_{int} is greater by ca. 30 kcal/mol when the bond is considered to arise from such a donor–acceptor interaction; this is a natural consequence of the system enjoying greater stabilization upon bond formation when starting from excited fragments. Because the principal bond type of interest in the present work is that exemplified by the donor–acceptor bond in $Me_3P{:}\!\rightarrow S$ (for which the singlet ground state in the donor, PMe_3, is vastly lower in energy than its first triplet excited state), we adopt the donor–acceptor fragment model for purposes of comparison. In a theoretical investigation of hypervalency, the phosphine−sulfide bond has been investigated previously by an incisive atoms in molecules analysis.[5]

From Table 3, it is of interest to note that the repulsive contribution ΔE_{Pauli} to the interaction energy is at a maximum when the sulfur atom is bonded to a carbon atom. However, the large ΔE_{Pauli} terms are offset by large attractive ΔE_{elstat} and ΔE_{orb} terms such that the largest overall interaction energy is found for thioformaldehyde, and also the *N*-heterocyclic carbene model system $SC(HNCH)_2$ has a greater ΔE_{int} than does $SPMe_3$. Interestingly, the orbital mixing contributions ΔE_{orb} to the interaction energy are very similar in magnitude for the pair $SC(HNCH)_2$ and $SPMe_3$, even when broken down into σ (A_1) and π components. There has been much interest in the ability of *N*-heterocyclic carbenes to engage in π interactions.[44,56] The model system $SC(HNCH)_2$ investigated herein derives 19% of its ΔE_{orb} from π interactions; this very same value is obtained for $SPMe_3$.

It can be inferred from Table 3 that the maximum of bonding to a terminal sulfur atom corresponds to a ΔE_{int} of ca. 200 kcal/mol in the donor–acceptor formalism, a value approached in both SCH_2 and $SNb(NH_2)_3$ cases. Analyzing the orbital contribution to these bonds reveals that the former is 32% due to π interactions, while the latter is due only 15% to π interactions. This is counter to what is anticipated on the basis of correspondence to formal double and triple

---

(51) Morokuma, K. *J. Chem. Phys.* **1971**, *55*, 1236–44.

(52) Ziegler, T.; Rauk, A. *Theor. Chim. Acta* **1977**, *46*, 1–10.

(53) Esterhuysen, C.; Frenking, G. *Theor. Chem. Acc.* **2005**, *113*, 294–294.

(54) Kovacs, A.; Esterhuysen, C.; Frenking, G. *Chem.—Eur. J.* **2005**, *11*, 1813–1825.

(55) Moore, C. E. *Atomic Energy Levels*; National Bureau of Standards: Washington, DC, 1949; Vol. *I*, Circular 467.

(56) Green, J. C.; Scurr, R. G.; Arnold, P. L.; Cloke, F. G. N. *Chem. Commun.* **1997**, 1963–1964.

(57) Balazs, G.; Gregoriades, L. J.; Scheer, M. *Organometallics* **2007**.

Table 4. Terminal Chalcogen Bond Strength Estimates as a Function of the Chalcogen, E[a]

E	HE−H[b]	P(n-Bu)$_3$[c]	IPr[d]	[**Mo**][e]	PhE−[**Mo**] (ratio)[e,f]
S	91	96	102	115	55 (2.09)
Se	80	75	77	87	52 (1.67)
Te	66	52	53	64	41 (1.56)

[a] All data are given in units of kcal/mol and are for all species in toluene solution; BDE estimates are considered reliable to within ± 3 kcal/mol. [b] Average HE−H single bond strength.[58] [c] Data for S−P(n-Bu)$_3$ were reported earlier;[21] values for terminal chalcogen bonds to P(n-Bu)$_3$ are identical to those for PCy$_3$ to within ± 1 kcal/mol, so these phosphines are used interchangeably in the text. [d] Data for the S−IMes bond were reported previously;[22] IMes and IPr here are assumed to be interchangeable with respect to the energies of their bonds to terminal chalcogen atoms.[43] [e] [**Mo**] here refers to Mo(N[t-Bu]Ar)$_3$. [f] Here, (ratio) is the ratio of the terminal E−Mo bond energy in EMo(N[t-Bu]Ar)$_3$ to the energy of the corresponding E−Mo bond in PhEMo(N[t-Bu]Ar)$_3$.

bonds, respectively. In addition, the contribution of ionic resonance structures to the bond energy as given by ΔE_{elstat} is actually greater for thioformaldehyde than for the niobium sulfide! The extent of covalency, as given by $\Delta E_{\text{orb}}/(\Delta E_{\text{orb}} + \Delta E_{\text{elstat}})$, is actually very similar for this pair of systems (62% for SNb(NH$_2$)$_3$ and 59% for SCH$_2$).

Another interesting case is the C_{3v} symmetric PS model complex, SPMo(NH$_2$)$_3$,[28] which is obtained formally by sulfur atom transfer to the terminal phosphide[57] PMo(NH$_2$)$_3$.[28] This system has the smallest ΔE_{int} of any of the systems studied here, even though the orbital contributions to the bonding exceed those in SPMe$_3$ by 6 kcal/mol. The extent of P−S bond covalency in SPMo(NH$_2$)$_3$ is very high, at 71% (as compared with 60% for SPMe$_3$), and its small interaction energy can be traced to a very small value of ΔE_{elstat}. It is interesting that SPMo(NH$_2$)$_3$ contains at once the most covalent and the weakest of the bonds to sulfur investigated herein.

Summary of Bond Strength Estimates. Thermochemical analysis of a specific reaction is generally best done by using derived enthalpic and entropic data directly without recourse to bond strength estimates. Nevertheless, bond strength data provide a simple and convenient means to estimate and understand reactions of interest. Data in Table 4 represent our best solution-phase estimates of bond strengths for three systems: EP(n-Bu)$_3$, the IPr-derived heavy urea analogs, and the terminal chalcogen complexes EMo(N[t-Bu]Ar)$_3$. Also included in Table 4 for reference are the average HE−H bond dissociation enthalpies and the PhE−Mo(N[t-Bu]Ar)$_3$ bond energy.[12]

The data in Table 4 reveal a relatively even change in bond strength, with bond energies to a given chalcogen increasing in the order P(n-Bu)$_3$ < IPr < Mo(N[t-Bu]Ar)$_3$ and with the chalcogens following the expected bond strength pattern that the heavier the chalcogen, the weaker are the bonds that it forms. All these terminal chalcogen systems have sufficiently strong values of the formal bond strength that the enthalpy of the reaction expressed in eq 20 is exothermic by over 30 kcal/mol.

$$A + EH_2 \rightarrow AE + H_2 \tag{20}$$

where A = P(n-Bu)$_3$, IPr, or Mo(N[t-Bu]Ar)$_3$.

The data in Table 4 permit a comparison between the formal single E−Mo bond in PhEMo(N[t-Bu]Ar)$_3$ and the correponding formal double bond in the terminal chacogen complexes EMo(N[t-Bu]Ar)$_3$. Of particular interest is the ratio of these two bond strengths, which decreases from 2.09 to 1.67 to 1.56 in going from S to Se to Te. This is in keeping with the propensity of terminally bonded chalcogen systems to dimerize or oligomerize (cf. eq 3). For the bulky EMo(N[t-Bu]Ar)$_3$ complexes, however, such dimerization is inhibited on steric grounds.

Concluding Remarks

This paper presents calorimetric data allowing a comparison of S, Se, and Te atom transfer reactions that yield compounds containing bonds between C, P, or Mo and a terminal chalcogen atom. Thermochemical data do not provide insight into the nature of the bonding in these terminal chalcogen molecules except insofar as the magnitude of the bond dissociation enthalpy is determined. In contrast, theoretical energy partitioning analysis provides detailed insight into the nature of the bonding interaction, while being less valuable for obtaining accurate absolute bond energies. This paper has endeavored to achieve a synergy between these two different approaches.

While not a dominant factor in the bonding, neither should π interactions in these systems be discounted.[44] The fact that the extent of the computed P−S bond covalency in SPMo(NH$_2$)$_3$ was very high—despite a relatively weak net interaction—makes it quite clear that the net bonding interaction to a terminal chalcogen substituent under any particular circumstance is the sum of a complex mix of interactions. The terminal chalcogen bonds studied here defy assignment of conventional integer bond orders. Those who wish to understand and utilize their reactivity “must go to the facts themselves for everything”.[59]

Acknowledgment. The authors are grateful for support of this work by the National Science Foundation (grants CHE-0719157 and CHE-0615743) and by the Department of Energy (grant DE-FG02-06ER15799). S.P.N. acknowledges support from the Ministerio de Educación y Cienca, ICREA, and the ICIQ Foundation.

Supporting Information Available: Crystallographic data in CIF file format for the structures of TePCy$_3$ and (μ-S)[Mo(N[t-Bu]Ar)$_3$]$_2$, as well as Figures S1 and S2. This material is available free of charge via the Internet at http://pubs.acs.org.

IC701611P

---

(58) NIST Webbook. http://webbook.nist.gov/.

(59) Cotton, F. A.; Wilkinson, G.; Gaus, P. L. *Basic Inorganic Chemistry*, 3rd ed.; J. Wiley: New York, 1995. The partial quote of F. Bacon (1620) given here is taken from the preface to the first edition.